Journal Name

ARTICLE

Elastomeric polyethylenes accessible via ethylene homo-polymerization using an unsymmetrical α-diimino-nickel catalyst

cccReceived 00th January 20xx,
Accepted 00th January 20xx

DOI: 10.1039/x0xx00000x

www.rsc.org/

Xinxin Wang,[a,b] Linlin Fan,[a,b] Yanping Ma,[b] Cun-Yue Guo,*[,a] Gregory A. Solan,*[,b,c] Yang Sun[b] and Wen-Hua Sun*[,b,d]

Five types of unsymmetrical bis(arylimino)acenaphthenes, 1-[2,4,6-$(CHPh_2)_3C_6H_2N$]-2-(ArN)$C_2C_{10}H_6$ (Ar = 2,6-Me_2Ph **L1**, 2,6-Et_2Ph **L2**, 2,6-i-Pr_2Ph **L3**, 2,4,6-Me_3Ph **L4**, 2,6-Et_2-4-MePh **L5**), each containing a single *N*-2,4,6-tribenzhydrylphenyl group, have been prepared and fully characterized. Interaction of **L1** – **L5** with (DME)$NiBr_2$ (DME = 1,2-dimethoxyethane) afforded the corresponding 1:1 nickel(II) bromide chelates, **L**$NiBr_2$ (**Ni1** – **Ni5**), in good yield. Distorted tetrahedral geometries are a feature of the X-ray structures of **Ni1** and **Ni3**; in solution broad paramagnetically shifted peaks are seen in the ^{1}H NMR spectra for all the nickel complexes. Upon activation with relatively low amounts of Et_2AlCl or Me_2AlCl (200 – 700 equivalents), **Ni1** – **Ni5** exhibited exceptionally high activities for ethylene polymerization (up to 1.07×10^7 g of PE (mol of Ni)$^{-1}h^{-1}$), displayed good thermal stability [2.97×10^6 g of PE (mol of Ni)$^{-1}h^{-1}$ even at 90 ºC] and produced hyperbranched polyethylenes. Dynamic mechanical analysis and stress-strain testing reveals that the polymeric materials possess good elastomeric recovery and high elongation at break, indicating a promising alternative material to thermoplastic elastomers (TPEs).

Introduction

Thermoset elastomers are experiencing an ever growing demand for applications in the automotive, gasket, hose and clothing industries.[1] Typical elastomers such as vulcanized rubber are amorphous materials that contain chemical cross-links that can suffer with problems associated with recycling, reprocessing and or/reusing.[2,3] As a valuable alternative to thermoset elastomers,[1] thermoplastic elastomers (TPEs), based on block copolymers and graft copolymers incorporating physical cross-links, have emerged in the field. Some examples of TPEs include miktoarm block, star-like block, regioirregular block and hyperblock copolymers. However, these materials are commonly synthesized by somewhat complicated multistep methods involving controlled/living radical polymerization (CRP) and living anionic polymerization making them time-consuming approaches.[4,5] As a more industrially promising and straightforward strategy, polyolefin block and graft copolymers can be prepared by the co-polymerization of ethylene with an α-olefin in the presence of a metallocene catalyst.[6] Elsewhere, late transition metal catalysts such as α-diimino nickel(II)- or palladium(II)-based systems have shown great potential in their ability to mediate the homo-polymerization of ethylene to form hyperbranched polyethylenes that are related in structure to TPEs.[7,8] To enhance the temperature stability of the nickel pre-catalysts (**A**, Chart 1),[7a,7b] a range of bis(arylimino)acenaphthene or related nickel halide derivatives have been disclosed that incorporate dibenzhydryl-substituted *N*-aryl groups (**B**,[9] **C**,[10] and **D**,[11] Chart 1). Significantly, **B** – **D** can not only operate efficiently at higher temperature but also afford polyethylenes that display higher branching contents at these temperatures.

In this work, we explore the use of a new family of benzhydryl-containing unsymmetrical bis(arylimino) acenaphthene-nickel(II) bromide complexes as pre-catalysts for the formation of hyperbranched polyethylenes at a range of temperatures up to 90 ºC (**E**, Chart 1). By installing a single 2,4,6-tribenzhydrylphenyl group as one *N*-aryl group, we additionally probe the effect on catalytic performance of modifying the steric and electronic properties of the second aryl group. Exceptional thermal stability and high activity is a feature of the polymerization catalysis, while hyperbranched structures with almost dendritic qualities are exhibited by the polyethylenes; a detailed investigation of the mechanical properties of these materials is also disclosed. In addition to the catalytic investigation and polymer studies, we also report the synthesis and characterization of all ligands and complexes.

[a] School of Chemistry and Chemical Engineering and CAS Research/Education Center for Excellence in Molecular Sciences, University of Chinese Academy of Sciences, Beijing 100049, China. E-mail: cyguo@ucas.ac.cn
[b] Key Laboratory of Engineering Plastics and Beijing National Laboratory for Molecular Sciences, Institute of Chemistry, Chinese Academy of Sciences, Beijing 100190, China. E-mail: whsun@iccas.ac.cn
[c] Department of Chemistry, University of Leicester, University Road, Leicester LE1 7RH, UK. E-mail: gas8@leicester.ac.uk
[d] State Key Laboratory for Oxo Synthesis and Selective Oxidation, Lanzhou Institute of Chemical Physics, Chinese Academy of Sciences, Lanzhou 730000, China.
Electronic Supplementary Information (ESI) available: Single edge notched tensile test and ^{13}C NMR of PEs. CCDC 1537069 and 1537070 for N**i1** and **Ni3**. See DOI: 10.1039/x0xx00000x
*On the occasion of 70th birthday of Professor Joachim W. Heinicke

Please do not adjust margins

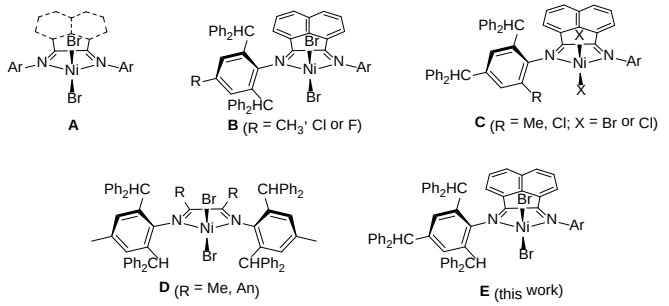

Chart 1 Development of α-diimino-nickel(II) halide pre-catalysts, **A** - **E**

Results and discussions

Synthesis and characterization of L1 – L5 and Ni1 – Ni5

The unsymmetrical 1,2-bis(arylimino)acenaphthenes, 1-[2,4,6-$(CHPh_2)_3C_6H_2N$]-2-(ArN)$C_2C_{10}H_6$ (Ar = 2,6-Me_2Ph **L1**, 2,6-Et_2Ph **L2**, 2,6-*i*-Pr_2Ph **L3**, 2,4,6-Me_3Ph **L4**, 2,6-Et_2-4-MePh **L5**), can be prepared in good yield by the condensation reaction of 2-(2,4,6-tribenzhydrylphenylimino)acenaphthylenone with the corresponding aniline in toluene at reflux (Scheme 1). The imine-ketone precursor is not commercially available and could be readily prepared by treating acenaphthylene-1,2-dione with 2,4,6-tribenzhydrylaniline in an ethanol/dichloromethane mixture at room temperature. **L1** – **L5** were characterized by ^{1}H/^{13}C NMR and IR spectroscopy as well as by microanalysis.

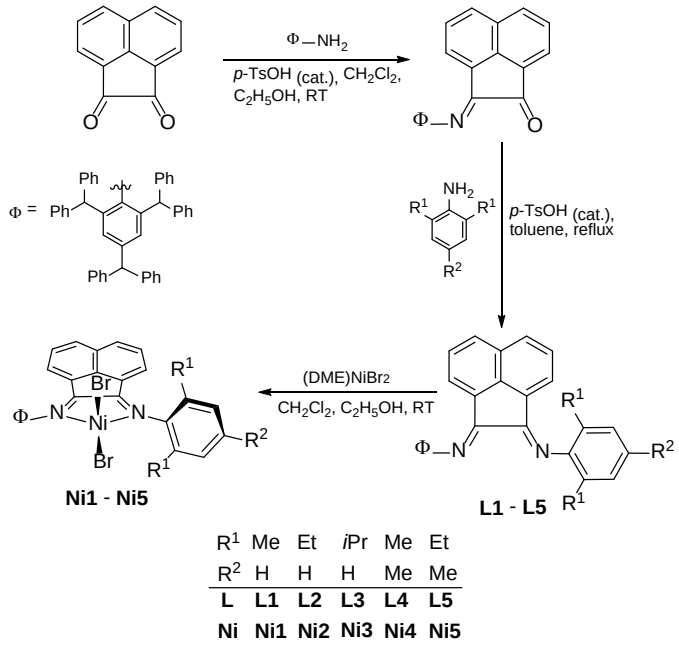

R^1	Me	Et	*i*Pr	Me	Et
R^2	H	H	H	Me	Me
L	**L1**	**L2**	**L3**	**L4**	**L5**
Ni	**Ni1**	**Ni2**	**Ni3**	**Ni4**	**Ni5**

Scheme 1 Synthesis of **L1** – **L5** and their nickel(II) bromide complexes **Ni1** – **Ni5**.

On reaction of **L1** – **L5** with (DME)$NiBr_2$ (DME = 1,2-dimethoxyethane) in dichloromethane gave their corresponding 1:1 nickel(II) bromide complexes, **Ni1** – **Ni5**, in good yields (Scheme 1). All the complexes have been characterized by ^{1}H NMR and IR spectroscopy as well as by microanalysis. In addition, **Ni1** and **Ni3** have been the subject of single crystal X-ray diffraction studies. In their FT-IR spectra, the stretching frequencies for the C=N bonds in **Ni1** – **Ni5** fall in the range 1648 – 1614 cm^{-1} which compares to 1668 – 1634 cm^{-1} for the free ligands; this lowering in wavenumber on complexation is consistent with the effective coordination between the nickel ion and the N_{imino} atoms. The ^{1}H NMR spectra for **Ni1** –**Ni5** are broad and paramagnetically shifted and appear between +30 to –16 ppm, chemical shifts characteristic of related tetrahedral Ni(II) complexes.[8h]

Single crystals of **Ni1** and **Ni3** were grown by layering dichloromethane solutions of the corresponding complex with diethyl ether. Their molecular structures are shown in Figs. 1 and 2; selected bond lengths and angles are collected in Table 1. **Ni1** and **Ni3** are closely related and will be discussed together. Each structure comprises a single nickel center bound by the two nitrogen donor atoms belonging to the unsymmetrical *N,N*-bis(arylimino)acenaphthene and by two bromide ligands to complete a geometry best described as distorted tetrahedral.[9] The key difference between **Ni1** and **Ni2** arises in the nature of the aryl group linked to imine-N1; in **Ni1** it is a 2,6-dimethylphenyl group while in **Ni3** it is a 2,6-diisopropylphenyl group.

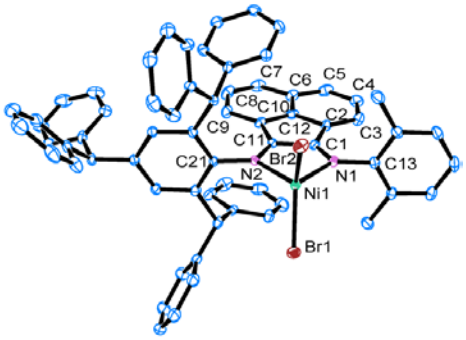

Fig. 1 ORTEP drawing of **Ni1** with thermal ellipsoids at a 30% probability level. Hydrogen atoms have been omitted for clarity.

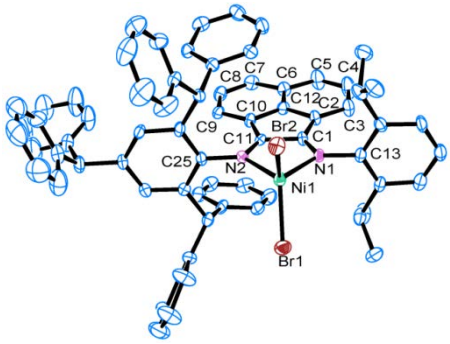

Fig. 2 ORTEP drawing of **Ni3** with thermal ellipsoids at a 30% probability level. Hydrogen atoms have been omitted for clarity.

The bite angles for the bidentate ligands are similar [N1-Ni1-N2: 83.7(2) (**Ni1**), 82.65(15)° (**Ni3**)], while the Br1-Ni-Br2 angle for **Ni1** is somewhat larger than that for **Ni3** [125.77(3) vs. 121.82(4)°]. Despite the inequivalent steric and electronic properties of the aryl groups linked to the imine nitrogen atoms in each structure, there are only minor differences in Ni-N bond distances with that involving the Ni1-N(2,4,6-tribenzhydrylphenyl) marginally longer in **Ni3** (Ni1-N1 2.041(4) vs. Ni1-N2 2.029(4) Å). The N1-C1 [1.272(9) Å (**Ni1**),

1.280(6) Å (**Ni3**)] and N2-C11 [1.299(9) Å (**Ni1**), 1.301(6) Å (**Ni3**)] bond distances are consistent with C=N double-bond character while the imine vectors are essentially co-planar with the acenaphthene unit. By contrast, the *N*-aryl rings in both structures are close to perpendicular with respect to the neighbouring imine vectors.

Table 1 Selected bond lengths (Å) and angles (°) for **Ni1** and **Ni3**

	Ni1		**Ni3**
	Bond lengths (Å)		
Ni(1)–Br(1)	2.3265(12)	Ni(1)–Br(1)	2.3466(9)
Ni(1)–Br(2)	2.3373(11)	Ni(1)–Br(2)	2.3346(8)
Ni(1)–N(1)	2.037(6)	Ni(1)–N(1)	2.029(4)
Ni(1)–N(2)	2.040(6)	Ni(1)–N(2)	2.041(4)
N(1)–C(1)	1.272(9)	N(1)–C(1)	1.280(6)
N(1)–C(13)	1.430(9)	N(1)–C(13)	1.449(6)
N(2)–C(11)	1.299(9)	N(2)–C(11)	1.301(6)
N(2)–C(21)	1.446(8)	N(2)–C(25)	1.446(5)
	Bond angles(°)		
N(1)–Ni(1)–N(2)	83.7(2)	N(1)–Ni(1)–N(2)	82.65(15)
Br(1)–Ni(1)–Br(2)	125.77(5)	Br(1)–Ni(1)–Br(2)	121.82(4)
N(1)–Ni(1)–Br(1)	111.37(16)	N(1)–Ni(1)–Br(1)	109.32(10)
N(2)–Ni(1)–Br(1)	110.16(14)	N(2)–Ni(1)–Br(1)	111.19(9)
N(1)–Ni(1)–Br(2)	107.50(16)	N(1)–Ni(1)–Br(2)	112.50(9)
N(2)–Ni(1)–Br(2)	110.35(15)	N(2)–Ni(1)–Br(2)	112.61(9)

Catalytic evaluation for ethylene polymerization

Co-catalyst screen using Ni1. In the first instance **Ni1** was employed as the test pre-catalyst and screened with a range of different aluminum-containing co-catalysts. In particular, seven different aluminum alkyls were evaluated namely methylaluminoxane (MAO), modified methylaluminoxane (MMAO), ethylaluminumdichloride ($AlEtCl_2$), ethylaluminumsesquichloride ($Et_3Al_2Cl_3$, EASC), trimethylaluminum (Me_3Al), triethylaluminum (Et_3Al), dimethylaluminum chloride (Me_2AlCl) and diethylaluminum chloride (Et_2AlCl). Typically the runs were performed at 30 ºC under 10 atmospheres of ethylene pressure; the results are summarized in Table 2 (runs 1-8). Apart from with EASC, good activities were achieved with all of the co-catalysts with **Ni1**/Me_2AlCl and **Ni1**/Et_2AlCl systems exhibiting the best performance characteristics (runs 7 and 8, Table 2). On the basis of these findings, Me_2AlCl and Et_2AlCl were selected as the co-catalysts for all subsequent screening (*vide infra*).

Catalytic optimization with Ni1 – Ni5/Me_2AlCl. With a view to ascertaining the optimal Al/Ni molar ratio, reaction temperature and reaction time, with Me_2AlCl as the co-catalyst, **Ni1** was again employed as the test pre-catalyst (Table 3). Firstly, the Al/Ni molar ratio was systematically varied with the temperature and pressure kept constant. At 30 ºC the catalytic activity gradually increased as the Al/Ni molar ratio was raised from 200 reaching a maximum at 700 (runs 1–6, Table 3). As this ratio was increased further up to 900, the activity was found to steadily drop (runs 7,8, Table 3).

Table 2 Identification of the most compatible co-catalyst using **Ni1** [a]

Run	Co-cat.	Al/Ni	Activity[b]	T_m[c]/ºC	M_w[d]/10^5 g·mol^{-1}	M_w/M_n[d]
1	MAO	2000	2.74	89.7	5.09	2.3
2	MMAO	2000	4.46	100.5	9.87	2.3
3	$EtAlCl_2$	400	1.97	101.3	3.49	2.1
4	EASC	400	trace		-	-
5	Et_3Al	400	0.29	98.9	4.17	2.8
6	Me_3Al	400	4.48	92.8	5.42	2.1
7	Me_2AlCl	400	9.95	69.9	4.88	2.4
8	Et_2AlCl	400	6.21	67.3	4.00	2.6

[a] Conditions: 2.0 μmol of **Ni1**; 30 mins; 30 ºC; 10 atm of ethylene; 100 mL toluene. [b] 10^6 g of PE (mol of Ni)$^{-1}$ h^{-1}. [c] Determined by DSC. [d] Determined by GPC.

Secondly, with the Al/Ni ratio set at 700, the reaction temperature was increased from 20 to 90 ºC (runs 6, 9–15, Table 3) with the catalytic activity reaching a peak of 1.07×10^7 g of PE (mol of Ni)$^{-1}$ h^{-1} at 30 ºC (run 6, Table 3). Above 30 ºC, the activities gradually decreased which can be attributed to partial deactivation of the active species with temperature.[8a,9] Nevertheless, even at 90 ºC **Ni1**/Me_2AlCl maintained a remarkably good level of 2.97×10^6 g of PE (mol of Ni)$^{-1}$ h^{-1} (run 15, Table 3). With regard to the molecular weight of the polyethylenes, this was found to decrease as the reaction temperature was raised from 30 to 90 ºC, in accord with more facile chain transfer and termination (runs 6, 9–15, Table 3 and Fig. 3).[10]

Thirdly, to explore the lifetime of the active species, the polymerization runs using **Ni1**/Me_2AlCl were conducted over different reaction times, namely 5, 10, 15, 30, 45 and 60 minutes (runs 8 and 16–20, Table 3). After 5 minutes (run 16, Table 3), the highest activity of all the runs was observed at 1.71×10^7 g of PE (mol of Ni)$^{-1}$ h^{-1}, likely reflecting the rapid generation of the active species. Subsequently, the catalytic activity steadily decreases and after 30 minutes it dropped by *ca.* 38% and by 60 minutes a further 32%. Nevertheless, the molecular weight of the polyethylene increases over the same period indicating that at longer run times there are still sufficient catalytic species to retain activity (Fig. 4).[9c,12] Similar partial deactivation of active sites over extended reaction times has been previously reported for related α-diimino-nickel catalysts.[8c,9]

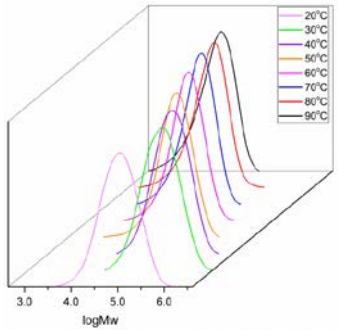

Fig. 3 GPC curves of the polyethylenes obtained using **Ni1**/Me_2AlCl at different temperatures (runs 6, 9–15 in Table 3)

Table 3. Ethylene polymerization runs using **Ni1 – Ni5**/Me_2AlCl [a]

Run	Pre-cat.	Al/Ni	*T*/°C	*t*/min	Activity[b]	T_m[c]/ºC	M_w[d]/10^5g·mol^{-1}	M_w/M_n[d]
1	**Ni1**	200	30	30	4.98	63.3	2.55	2.2
2	**Ni1**	300	30	30	8.51	61.3	4.68	2.3
3	**Ni1**	400	30	30	9.95	69.9	4.88	2.4
4	**Ni1**	500	30	30	10.12	53.6	4.20	2.2
5	**Ni1**	600	30	30	10.41	63.9	6.28	2.4
6	**Ni1**	700	30	30	10.70	59.6	4.44	2.1
7	**Ni1**	800	30	30	8.21	62.0	4.57	2.3
8	**Ni1**	900	30	30	7.34	55.5	3.17	2.1
9	**Ni1**	700	20	30	4.98	98.5	1.56	2.3
10	**Ni1**	700	40	30	5.75	55.9	2.70	2.0
11	**Ni1**	700	50	30	3.98	37.5	1.17	1.9
12	**Ni1**	700	60	30	3.82	28.1	0.77	2.0
13	**Ni1**	700	70	30	3.77	25.4	0.49	2.0
14	**Ni1**	700	80	30	3.65	24.0	0.33	2.2
15	**Ni1**	700	90	30	2.97	14.2	0.17	2.2
16	**Ni1**	700	30	5	17.12	77.5	0.39	2.3
17	**Ni1**	700	30	10	15.85	87.4	0.92	2.1
18	**Ni1**	700	30	15	13.34	71.1	1.98	1.8
19	**Ni1**	700	30	45	9.53	81.6	6.85	2.6
20	**Ni1**	700	30	60	7.23	84.2	6.94	2.4
21	**Ni2**	700	30	30	6.60	58.1	6.41	2.4
22	**Ni3**	700	30	30	10.93	43.5	4.91	2.5
23	**Ni4**	700	30	30	8.06	82.5	8.72	3.1
24	**Ni5**	700	30	30	5.59	53.2	6.53	2.3
25[e]	**Ni1**	700	30	30	0.52	10.2	0.25	2.8
26[f]	**Ni1**	700	30	30	3.19	59.1	3.59	2.4

[a] Conditions: 2.0 μmol of catalyst, ethylene pressure 10 atm, total volume 100 mL. [b] 10^6 g of PE (mol of Ni)$^{-1}$ h^{-1}. [c] Determined by DSC. [d] Determined by GPC. [e] Ethylene pressure 1 atm. [f] Ethylene pressure 5 atm.

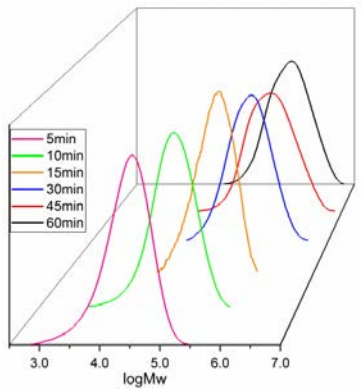

Fig. 4 GPC curves of the polyethylenes obtained using **Ni1**/Me_2AlCl at different run times (runs 8 and 16–20 in Table 3)

In terms of the ethylene pressure, both the catalytic activity of **Ni1**/Me_2AlCl and the molecular weight of the polymer were greatly affected by pressure variations. With the Al/Ni ratio fixed at 700 and the reaction temperature at 30 ºC the polymerization runs were conducted under three different pressures, 1, 5 and 10 atmospheres (runs 8, 25, 26 in Table 3). As expected higher molecular weight polyethylene was produced at higher ethylene pressure.[8a] Likewise the catalytic activities were superior at higher pressures.

With the optimal conditions for **Ni1**/Me_2AlCl established with an Al/Ni molar ratio of 700, a temperature of 30 ºC and 10 atmospheres of ethylene pressure, **Ni2**, **Ni3**, **Ni4** and **Ni5** were investigated under these conditions (runs 21–24, Table 3). All pre-catalysts displayed good activities [range: 5.59 – 10.93 × 10^6 g of PE (mol of Ni)$^{-1}$ h^{-1}] and when put together with **Ni1** were found to decrease in the order **Ni3** [2,6-di(*i*-Pr)] ≈ **Ni1** [2,6-di(Me)] > **Ni4** [2,4,6-tri(Me)] > **Ni2** [2,6-di(Et)] > **Ni5** [2,6-di(Et)-4-Me]. Clearly both electronic and steric effects imparted by this second *N*-aryl group are influential but the trends are far from clear. Notably, the presence of the *para*-methyl groups in **Ni4** and **Ni5** appears to have a negative effect on catalytic activity when compared with their *para*-hydrogen counterparts, **Ni1** and **Ni2**, respectively.

Catalytic optimization with Ni1–Ni5/Et_2AlCl. As a separate study we also explored the use of Et_2AlCl as the co-catalyst. As before, **Ni1** was used to optimize the polymerization parameters including the Al/Ni molar ratio, reaction temperature and reaction time (Table 4). At 30 ºC, the catalytic activities were measured at molar ratios of Al/Ni between 100 and 500 (runs 1-5, Table 4). Unexpectedly, a peak in activity was observed with only 200 equivalents of Et_2AlCl (run 2, Table 4). It

is unclear as to why less Et_2AlCl is needed to achieve the optimal activity for **Ni1** when compared with Me_2AlCl (*vide supra*).

Table 4. Ethylene polymerization runs using **Ni1 – Ni5**/Et_2AlCl [a]

Run	Pre-cat.	Al/Ni	*T*/°C	*t*/min	Activity[b]	T_m[c]/°C	M_w[d]/10^5g·mol^{-1}	M_w/M_n[d]
1	**Ni1**	100	30	30	5.31	66.9	5.09	2.8
2	**Ni1**	200	30	30	8.89	60.8	6.83	2.8
3	**Ni1**	300	30	30	7.96	62.3	6.01	2.4
4	**Ni1**	400	30	30	6.21	67.3	5.41	2.6
5	**Ni1**	500	30	30	4.02	58.7	4.00	2.5
6	**Ni1**	200	20	30	8.54	96.9	4.77	2.3
7	**Ni1**	200	40	30	6.39	55.6	3.74	2.4
8	**Ni1**	200	50	30	3.85	34.3	3.45	1.8
9	**Ni1**	200	60	30	3.76	28.5	2.68	2.0
10	**Ni1**	200	70	30	3.65	22.3	2.24	2.0
11	**Ni1**	200	80	30	3.47	20.3	1.73	1.9
12	**Ni1**	200	90	30	2.70	13.2	1.30	2.1
13	**Ni1**	200	30	5	13.52	63.8	3.24	2.4
14	**Ni1**	200	30	10	12.26	64.7	3.81	2.3
15	**Ni1**	200	30	15	10.79	55.9	4.48	2.3
16	**Ni1**	200	30	45	7.94	64.8	5.02	2.4
17	**Ni1**	200	30	60	6.89	60.7	4.66	2.4
18	**Ni2**	200	30	30	8.46	43.5	7.72	2.3
19	**Ni3**	200	30	30	9.46	51.6	5.87	2.0
20	**Ni4**	200	30	30	8.97	60.9	4.40	2.4
21	**Ni5**	200	30	30	7.61	60.2	4.92	2.2
22[e]	**Ni1**	200	30	30	0.34	11.3	0.44	2.3
23[f]	**Ni1**	200	30	30	2.26	58.7	5.48	2.0

[a] Conditions: 2.0 μmol of catalyst, ethylene pressure 10 atm, total volume 100 mL. [b] 10^6 g of PE (mol of Ni)$^{-1}$ h^{-1}. [c] Determined by DSC. [d] Determined by GPC. [e] Ethylene pressure 1 atm. [f] Ethylene pressure 5 atm.

With the Al/Ni ratio set at 200, the temperature of the runs using **Ni1**/Et_2AlCl was varied between 20 and 90 ºC (runs 2, 6–12, Table 4). Inspection of the data reveals a maximum in activity of 8.89 × 10^6 g of PE (mol of Ni)$^{-1}$ h^{-1} at 30 ºC (run 2, Table 3) which is mirrored in the temperature study using Me_2AlCl as co-catalyst. In the same way, **Ni1**/Et_2AlCl retains good activity of 2.70 × 10^6 g of PE (mol of Ni)$^{-1}$ h^{-1} at temperatures as high as 90 ºC (run 12, Table 4). As regards the polyethylenes, higher molecular weights were achieved at lower reaction temperatures in a manner similar to that observed elsewhere[9] and with the earlier study performed in this work (runs 2, 6–12, Table 4, Fig. 5).

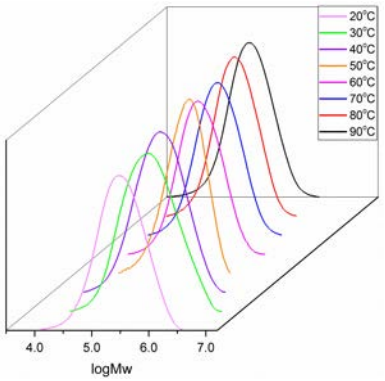

Figure 5. GPC curves of the polyethylenes obtained using **Ni1**/Et_2AlCl at different temperatures (runs 2, 6–12 in Table 4)

Lifetime studies were also conducted on **Ni1**/Et_2AlCl with the reaction parameters fixed at 30 ºC and an Al/Ni ratio of 200 (runs 2, 13–17, Table 4). A maximum in activity at 13.43 × 10^6 g of PE (mol of Ni)$^{-1}$ h^{-1} was again seen after 5 minutes which gradually dropped to 6.89 × 10^6 g of PE (mol of Ni)$^{-1}$h^{-1} after 60 minutes. As with **Ni1**/Me_2AlCl the active species was formed quickly and then underwent deactivation over time.

Finally, using the optimized conditions [Al/Ni ratio = 200, 30 °C, 10 atmospheres ethylene and 30 minute run time], **Ni2**, **Ni3**, **Ni4** and **Ni5** were all additionally investigated using Et_2AlCl as co-catalyst (runs 18–21, Table 3). All pre-catalysts displayed good activities [range: 7.61 – 9.46 × 10^6 g of PE (mol of Ni)$^{-1}$ h^{-1}] but fall in a narrower range when compared with the results obtained using Me_2AlCl. When put alongside **Ni1**, they decrease in the order **Ni3** [2,6-di(*i*-Pr)] > **Ni4** [2,4,6-tri(Me)] ≈ **Ni1** [2,6-di(Me)] > **Ni2** [2,6-di(Et)] > **Ni5** [2,6-di(Et)-4-Me]. Indeed the order of activities is similar to that observed with the Me_2AlCl-promoted systems with **Ni3** falling at the top end of the range and **Ni5** at the bottom with some variation evident in the middle.

Structural properties of the polyethylenes

To determine the branching content of the polymers, both DSC and ^{13}C NMR spectroscopic studies were undertaken. It was found that most of the melting temperatures (T_m) for the polymers were lower than 80 ºC, consistent with a high branching content.[8e,8f] To support this observation, two samples of polyethylene prepared using **Ni1** in combination with the two different co-catalysts, Me_2AlCl (run 6, Table 3) and Et_2AlCl (run 2, Table 4), were characterized by high temperature

^{13}C NMR spectroscopy (Figs. 6 and 7); the signals were assigned on the basis of previous reports and are listed in Tables 5 and 6.[13] The polyethylene obtained using **Ni1**/Me_2AlCl (run 6 in Table 3) contains 125 branches/1000 carbons, with the predominant types being methyl (65%), ethyl (4.1%), propyl (5.5%), butyl (8.8%) and longer chains (11%) as well as amyl chains (5.3%).

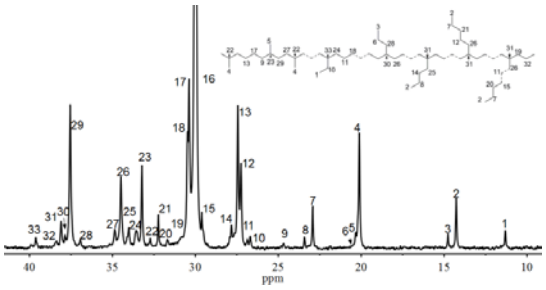

Fig. 6 ^{13}C NMR spectrum of the polyethylene sample obtained using **Ni1**/Me_2AlCl (run 6, Table 3)

Table 5 Branching analysis of the polyethylene sample obtained using **Ni1**/Me_2AlCl (run 6, Table 3)[a]

Peak No.	Chemical shift	Integral exp.	Branching content		Relative percentage
1	11.31	1	N_M	6.40	45.34%
2	14.27	2.63	$N_{M(1,4)}$	1.40	9.91%
3	14.77	0.7	$N_{M(1,5)}$	0.30	2.12%
4	19.86	7.15	$N_{M(1,6)}$	1.06	7.51%
5	20.12	1.07	N_E	0.58	4.10%
6	20.33	0.13	N_P	0.78	5.52%
7	22.93	2.09	N_B	1.25	8.82%
8	23.42	0.51	N_A	0.75	5.31%
9	24.67	0.3	N_L	1.01	7.15%
10	26.69	0.8	$N_{L(1,4)}$	0.60	4.22%
11	27.25	6.75			
12	27.44	9.1	[E]	42.17	
13	27.83	2.12	[R]	14.12	100%
14	29.53	1.15			
15	29.61	1.64	Total branching		
16	30	86.09	=125		
17	30.38	10.87	Branches/1000C		
18	30.48	7.08			
19	31.68	0.58	Methyl branches		64.88%
20	32.23	1.75	Ethyl branches		4.10%
21	32.72	0.75	Propyl branches		5.52%
22	33.22	5.16	Butyl branches		8.82%
23	33.57	2.1	Amyl branches		5.31%
24	33.83	0.27	Longer branches		11.37%
25	34.01	1.98			
26	34.49	6			
27	34.86	1.75			
28	36.94	0.78			
29	37.55	11.08			
30	37.86	0.76			
31	38.1	1.94			
32	38.37	0.9			
33	39.62	0.8			

[a] Determined by ^{13}C NMR spectroscopy.

In comparison, the polyethylene obtained using the **Ni1**/Et_2AlCl (run 2 in Table 4) revealed 135 branches/1000 carbons, with the main types of branch being methyl (84.4%) and ethyl (5.6%) as well as longer chain branches (10%). It is noteworthy that highly branched polyethylenes are common feature of the materials obtained using nickel-based catalytic systems due to the ease of chain isomerization.[14] Furthermore, it should also be noted that the microstructural properties of the polyethylene was affected by temperature (see Fig. S1-S3 and Table S1-S3).

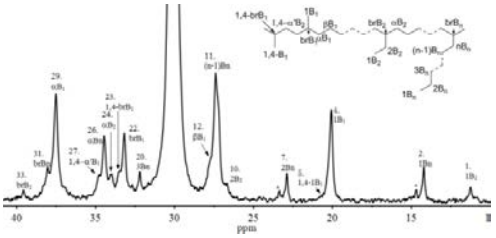

Fig. 7 ^{13}C NMR spectrum of the polyethylene sample obtained using **Ni1**/Et_2AlCl (run 2, Table 4)

Table 6 Branching analysis of the polyethylene sample obtained using **Ni1**/Et_2AlCl (run 2, Table 4)[a]

Peak No.	Chemical shift	Integral exp.	Branching content		Relative percentage
1	11.25	1	N_M	21.87	76.67%
2	14.21	2.46	$N_{M(1,4)}$	2.20	7.72%
3	14.65	0	$N_{M(1,5)}$	0.00	0.00%
4	19.86	0	$N_{M(1,6)}$	0.00	0.00%
5	20.07	10.17	N_E	1.60	5.62%
6	20.33	0	N_P	0.00	0.00%
7	22.89	1.81	N_B	0.00	0.00%
8	23.35	0	N_A	0.00	0.00%
9	24.67	0	N_L	2.85	9.99%
10	26.68	2.43	$N_{L(1,4)}$	0.00	0.00%
11	27.25	0			
12	27.4	23.35	[E]	77.38	
13	27.83	0	[R]	28.53	100%
14	29.53	0			
15	29.61	0	Total branching		
16	30	157.61	= 135		
17	30.38	0	Branches/1000C		
18	30.48	0			
19	31.68	0	Methyl branches		84.39%
20	32.2	2.85	Ethyl branches		5.62%
21	32.72	0	Propyl branches		0.00%
22	33.18	6.57	Butyl branches		0.00%
23	33.51	3.03	Amyl branches		0.00%
24	33.98	3.44	Long branches		9.99%
25	34.01	0			
26	34.46	6.3			
27	34.82	2.89			
28	36.94	0			
29	37.51	13.73			
30	37.86	0			
31	38.04	4.48			
32	38.37	0			
33	39.56	0.66			

[a] Determined by ^{13}C NMR spectroscopy.

Mechanical properties of the polyethylenes

To examine the mechanical properties of the polymeric materials, five samples were selected that were generated at five different run temperatures (20, 30, 40, 80 and 90 °C) using the same catalyst. Specifically samples PE-20, PE-30, PE-40, PE-80 and PE-90, obtained using **Ni1**/Et_2AlCl in runs 2, 6, 7, 11 and 12 in Table 4, were subjected to dynamic mechanical analysis (DMA) and stress-strain testing. In addition, notched samples of PE-30, PE-40 and PE-80 denoted *N*-PE-30, *N*-PE-40, *N*-PE-80 were also investigated as part of a single edge notched tensile test (SENT).[15]

Table 7 Selected properties of PE-20, PE-30, PE-40, PE-80 and PE-90 along with *N*-PE-30, *N*-PE-40 and *N*-PE-80

Entry	*T*/°C	T_m[a]/°C	M_w[b]/10^5 g·mol^{-1}	Branches[c]/1000Cs	X_c[a]/%	Stress[d]/MPa	Strain[d]/%
PE-20	20	96.9	4.77	106	20.7	13.52	218.3
PE-30	30	60.8	6.83	135	14.9	8.03	508.0
N-PE-30	30	60.8	6.83	135	14.9	2.90	83.3
PE-40	40	55.6	3.74	145	12.9	6.25	518.9
N-PE-40	40	55.6	3.74	145	12.9	2.31	99.4
PE-80	80	20.3	1.73	171	3.2	1.81	731.0
N-PE-80	80	20.3	1.73	171	3.2	0.97	645.5
PE-90	90	13.2	1.30	179	0.5	0.35	118.9

[a] Determined by DSC;$X_c=\Delta H_f(T_m)/\Delta H_f^o(T_m^o)$; $\Delta H_f^o(T_m^o) = 248.3$ Jg^{-1}.[16][b] Determined by GPC. [c] Determined by FT-IR.[17] [d] Determined using a universal tester.

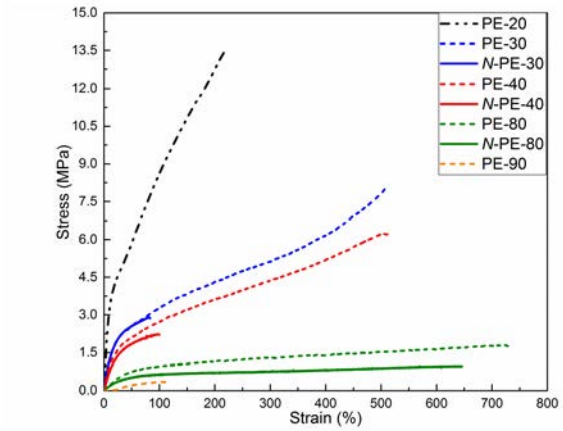

Fig. 8 Stress-strain curves for PE-20 – PE-90 along with notched samples *N*-PE-30, *N*-PE-40 and *N*-PE-80.

Firstly the monotonic tensile stress-strain data were recorded at 20 ºC on samples PE-20, PE-30, PE-40, PE-80 and PE-90 (Fig. 8). Each mechanical test was performed with five specimens in order to achieve consistent results. The lowest ultimate tensile stress (0.35 MPa) and strain at break (118.9%) was observed for PE-90, and this can be attributed to the material being almost amorphous at the measurement temperature. It was apparent that the absence of elasticity was caused by poor crystallinity, which was in-turn related to the high branching content. As the crystallinity gradually improved in PE-80 to 3.2%, the ultimate tensile stress and elongation at break both increased to 1.81 MPa and 731.0%, respectively. Raising the crystallinity still higher from 12.9 to 20.7% (PE-40 to PE-20), resulted in the ultimate tensile stress increasing further from 6.25 to 13.52 MPa. By contrast, the elongation at break decreased from 518.9 to 218.3% during this crystallinity transition. These observations indicate that the tensile properties of the polyethylene samples were significantly influenced by the branching architectures as well as the crystallinity.[18]

Secondly, the monotonic tensile stress-strain data of the single edge notched samples *N*-PE-30, *N*-PE-40 and *N*-PE-80 (pre-cut to a length of roughly 1 mm, Figs. S4-S6) were compared with PE-30, PE-40 and PE-80 (Fig. 8). With a single edge notch, the mechanical properties of all the *N*-PEs decreased when compared with the corresponding PE samples. For example, the ultimate tensile stress of *N*-PE-30 and *N*-PE-40 both decreased to 2.90 and 2.31 MPa from 8.03 and 6.25 MPa in PE-30 and PE-40. Similarly the elongation at break in *N*-PE-30 and *N*-PE-40 decreased significantly to 83.3 and 99.4% from 508.0 and 518.9%, respectively. Surprisingly, even the ultimate tensile stress in *N*-PE-80 decreased to 0.97 MPa from 1.81 MPa in PE-80, while the elongation at break in *N*-PE-80 at 645.5% compared favourably to the 731.0% seen in PE-80. These observations suggest that the high branching content of these polyethylenes leads to high physical cross-links which manifests itself in good tear resistance.[15]

Thirdly, the stress-strain recovery tests, recorded at -10 and 30 °C, were performed on PE-20, PE-40 and PE-80 by dynamic mechanical analysis (DMA) (Fig. 9). Each recovery test involved 10 cycles to allow testing for elastic extenuation with the exception of PE-80 at 30 °C; in this case the test temperature was above its T_m (20.3 ºC). Nevertheless this latter test revealed good tensile properties for the material with the strain exceeding the detection limit of the instrument (400%) after 3 cycles. In general, the results show that the elastic recovery decreased little and the samples could maintain elasticity after 10 cycles. As the temperature increased from −10 to 30 ºC the elastic recovery of PE-30 increased from 43 to 59%. Similarly the elastic recovery of PE-40 increased from 51 to 67% and the elastic recovery of PE-80 increased from 76 to 84%. At the same time the value of Young's moduli of PE-30 decreased significantly from 20.8 to 11.2 MPa. Likewise, the value of the Young's moduli of PE-40 decreased from 13.3 to 7.1 MPa, while the value of Young's moduli of PE-80 decreased from 3.5 to 0.6 MPa. This temperature dependence indicates that the elastomeric properties of the polyethylene samples were mainly influenced by the crystallinity rather than their molecular weight and molecular weight distribution.[18] Overall, these hyperbranched polyethylenes exhibit good tensile strength and elastic recovery, properties characteristic of thermoplastic elastomers (TPEs). Furthermore, the sample

obtained at high temperature (*N*-PE-80) showed good tear resistance.

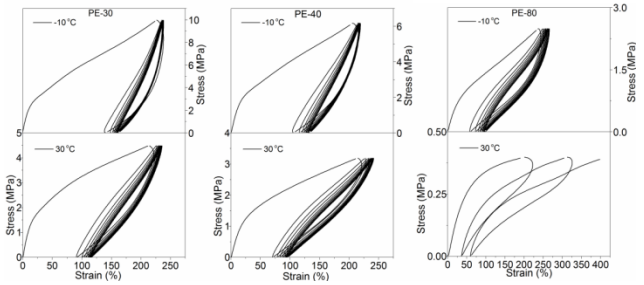

Fig. 9 Stress-strain recovery tests for PE-30, PE-40 and PE-80 at -10 and 30 °C

Conclusions

A series of unsymmetrical 1-(2,4,6-tribenzhydrylimino)-2-aryliminoacenaphthene-nickel(II) bromides was prepared and fully characterized by FT-IR spectra, elemental analysis, NMR spectroscopy as well as by single crystal X-ray diffraction. Upon activation with relatively low amounts of Et_2AlCl or Me_2AlCl, all the nickel complexes exhibited high activities even at 90 ºC (2.97×10^6 g of PE (mol of Ni)$^{-1}$ h^{-1}) for ethylene polymerization, affording hyperbranched polyethylenes. Notably, these polymeric materials displayed properties characteristic of thermoplastic elastomers (TPEs) and show great promise as potential alternatives to elastomeric ethylene copolymers.

Experimental

General procedure

All manipulations of air and/or moisture sensitive compounds were carried out under a nitrogen atmosphere using standard Schlenk techniques. All solvents were heated to reflux and purified under a nitrogen atmosphere before use. Methylaluminoxane (MAO, 1.46 M in toluene) and modified methylaluminoxane (MMAO, 1.93 M in heptane, 3A) were purchased from Akzo Nobel Corp. Diethylaluminum chloride (Et_2AlCl, 0.79 M in toluene), dimethylaluminum chloride (Me_2AlCl, 1.0 M in toluene), ethylaluminum dichloride ($AlEtCl_2$, 1.44 M in toluene) and ethylaluminumsesquichloride ($Et_3Al_2Cl_3$, EASC, 0.87 M in toluene) were purchased from Acros Chemical. Trimethylaluminum (Me_3Al, 1.0 M in toluene) and triethylaluminum (Et_3Al, 1.0 M in toluene) were purchased from Aldrich Chemical. High-purity ethylene was purchased from Beijing Yanshan Petrochemical Co. and used as received. Other reagents were purchased from Aldrich, Acros or local suppliers. ^{1}H and ^{13}C NMR spectra were recorded on a Bruker DMX 400 MHz instrument at ambient temperature using TMS as an internal standard; δ values were given in ppm and J values in Hz. FT-IR spectra were recorded on a Perkin-Elmer System 2000 FT–IR spectrometer. Elemental analyses were carried out using a Flash EA 1112 microanalyzer. Molecular weights (Mw) and molecular weight distributions (MWD) of the polyethylene were determined using a PL-GPC220 at 150 ºC with 1,2,4-trichlorobenzene as the solvent. The thermograms for the crystallization and melt process were recorded using differential scanning calorimeter (DSC, TA-Q2000) under a nitrogen atmosphere. Typically, a polyethylene sample of about 5.0 mg was heated to 150 ºC at a heating rate of 20 ºC min^{-1}, and kept for 5 min at 150 ºC to remove the thermal history and then cooled at a rate of 20 ºC min^{-1} to –20 ºC. ^{13}C NMR spectra of the polyethylene were recorded on a Bruker DMX 300 MHz instrument at 135 ºC in deuterated 1,2-dichlorobenzene with TMS as an internal standard. The stress-strain curves were obtained using a universal tester (Instron 1122, UK). The stress-strain recovery tests at different temperatures were carried out by dynamic mechanical analyzer (DMA, DMA800, TA) under controlled force mode.

Syntheses and characterization

2-(2,4,6-Tribenzhydrylphenylimino)acenaphthylenone. To a mixture of 2,4,6-tribenzhydrylaniline (5.81 g, 10 mmol), acenaphthylene-1,2-dione (1.82 g, 10 mmol) and a catalytic amount of *p*-toluenesulfonic acid (0.90 g) was added both dichloromethane (250 mL) and ethanol (30 mL) and the resulting solution stirred at room temperature overnight. All volatiles were removed under reduced pressure and the residue purified by alumina column chromatography (50/1 petroleum ether/ethyl acetate) to give the title compound as a red powder (4.50 g, 60%). Mp: 186–188 ºC. ^{1}H NMR (400 MHz, $CDCl_3$, TMS): *δ* (ppm) 8.01 (m, 2H), 7.70 (m, 2H), 7.21–7.27 (m, 5H), 7.10–7.19 (m, 8H), 7.01–7.03 (m, 5H), 6.93–6.99 (m, 5H), 6.73–6.75 (m, 7H), 6.49–6.53 (m, 2H), 6.36 (m, 2H), 5.41 (s, 3H). ^{13}C NMR ($CDCl_3$, 100 MHz, ppm): *δ* 189.6, 162.7, 146.9, 144.2, 142.9, 142.5, 141.6, 139.3, 131.8, 130.1, 129.9, 129.6, 129.4, 129.2, 128.9, 128.4, 128.1, 128.0, 127.7, 127.5, 127.0, 126.5, 126.1, 125.7, 125.4, 123.9, 121.5, 56.3, 56.1, 52.5, 52.2.

Synthesis of 1-(2,4,6-tribenzhydrylphenylimino)-2-aryliminoacenaphthenes, L1 – L5

L1. 1-(2,4,6-Tribenzhydrylphenylimino)acenaphthylenone (0.74 g, 1.0 mmol), 2,6-dimethylaniline (0.14 g, 1.2 mmol) and a catalytic amount of *p*-toluenesulfonic acid (0.10 g) were stirred and heated to reflux in toluene (50 mL) for 8 h. The solution was concentrated under reduced pressure and the resulting residue purified by alumina column chromatography (50/1 petroleum ether/ethyl acetate) to afford **L1** as a yellow powder (0.26 g, 31%). Mp: 215–217 ºC. ^{1}H NMR (400 MHz, $CDCl_3$, TMS): *δ*(ppm) 7.69 (d, *J* = 8 Hz, 1H), 7.52 (d, *J* = 8 Hz, 1H), 7.27–7.30 (m, 6H), 7.12–7.23 (m, 10H), 7.05–7.09 (m, 5H), 6.98–7.00 (m, 4H), 6.90–6.93 (m, 1H), 6.82–6.84 (m, 4H), 6.76 (s, 2H), 6.49–6.53 (m, 5H), 6.32–6.36 (m, 2H), 5.61 (s, 2H), 5.43 (s, 1H), 2.22 (s, 6H). ^{13}C NMR ($CDCl_3$, 100 MHz, ppm): *δ* 163.8, 161.3, 149.3, 147.7, 144.3, 143.2, 142.6, 141.6, 139.9, 138.7, 132.3, 129.8, 129.7, 129.5, 129.3, 129.2, 129.1, 128.8, 128.7, 128.6, 128.4, 128.3, 128.1, 128.0, 127.6, 127.4, 126.6, 126.5, 126.0, 125.3, 124.8, 124.2, 123.7, 121.7, 56.3, 52.3, 18.1. FT-IR (cm^{-1}): 3025 (m), 2863 (m), 1668 (*ν* (C=N), m), 1638 (*ν* (C=N), m), 1594 (m), 1493 (s), 1442 (s), 1257 (m), 1229 (w), 1201 (w), 1126 (w), 1077 (m), 1031 (m), 921 (w), 831 (s), 779 (s), 759 (m), 740 (m), 694 (s). Anal. Calcd. For $C_{65}H_{50}N_2$ (859.11): C, 90.87; H, 5.87; N, 3.26. Found: C, 90.64; H, 6.03; N, 3.23.

L2. Based on the method described for **L1**, **L2** was prepared by the reaction of 1-(2,4,6-tribenzhydrylphenylimino)acenaphthylenone (0.74 g, 1.0 mmol) with 2,6-diethylaniline (0.16 g, 1.2 mmol) in the presence of *p*-toluenesulfonic acid (0.10 g) and isolated as a yellow powder (0.32 g, 37%). Mp: 187–189 ºC. ^{1}H NMR (400 MHz, $CDCl_3$, TMS): δ (ppm) 7.69 (d, J = 8 Hz, 1H), 7.53 (d, J = 8.0 Hz, 1H), 7.18–7.26 (m, 16H), 7.05–7.07 (m, 5H), 6.99–7.02 (m, 4H), 6.86–6.90 (m, 1H), 6.83–6.85 (m, 4H), 6.78 (s, 2H), 6.50–6.54 (m, 5H), 6.33–6.37 (m, 2H), 5.63 (s, 2H), 5.45 (s, 1H), 2.70 (m, 2H), 2.54 (m, 2H), 1.19 (t, J = 7.6 Hz, 6H). ^{13}C NMR ($CDCl_3$, 100 MHz, ppm): δ 163.8, 161.5, 148.3, 147.7, 144.8, 144.3, 143.4, 142.6, 141.6, 140.1, 140.0, 138.7, 132.6, 132.3, 130.7, 129.8, 129.7, 129.6, 129.4, 129.3, 129.2, 129.1, 129.0, 128.8, 128.6, 128.4, 128.1, 127.9, 127.8, 127.6, 127.2, 126.7, 126.5, 126.2, 126.0, 125.9, 125.7, 125.4, 124.3, 124.1, 122.2, 56.3, 56.1, 52.4, 52.2, 24.5, 14.3. FT-IR (cm^{-1}): 3024 (m), 2866 (m), 1665 (*v* (C=N), m), 1636 (*v* (C=N), m), 1594 (m), 1493 (s), 1444 (s), 1254 (m), 1199 (w), 1127 (w), 1077 (m), 1031 (m), 922 (w), 831 (m), 780 (s), 740 (m), 694 (s). Anal. Calcd. For $C_{67}H_{54}N_2$ (887.16): C, 90.71; H, 6.14; N, 3.16. Found: C, 90.49; H, 6.37; N, 3.03.

L3. Based on the method described for **L1**, **L3** was prepared by the reaction of 1-(2,4,6-tribenzhydrylphenylimino)acenaphthylenone (0.74 g, 1.0 mmol) with 2,6-diisopropylaniline (0.19 g, 1.2 mmol) in the presence of *p*-toluenesulfonic acid (0.10 g) and isolated as a yellow powder (0.32 g, 35%). Mp: 211–213 ºC. ^{1}H NMR (400 MHz, $CDCl_3$, TMS): δ(ppm) 7.67 (d, J = 8.0 Hz, 1H), 7.50 (d, J = 8.4 Hz, 1H), 7.28 (m, 3H), 7.21–7.24 (m, 7H), 7.18–7.20 (m, 6H), 7.06–7.09 (m, 5H), 6.98–7.02 (m, 4H), 6.85–6.88 (m, 1H), 6.81–6.83 (m, 4H), 6.77 (s, 2H), 6.43–6.51 (m, 5H), 6.33–6.35 (m, 2H), 5.63 (s, 2H), 5.45 (s, 1H), 2.16 (m, 2H), 1.29 (d, J = 6.8 Hz, 6H), 1.02 (d, J = 6.8 Hz, 6H). ^{13}C NMR ($CDCl_3$, 100 MHz, ppm): δ 163.9, 161.9, 147.8, 147.1, 144.8, 144.3, 143.5, 142.6, 141.5, 140.3, 140.0, 138.8, 135.7, 132.5, 132.4, 129.8, 129.7, 129.6, 129.4, 129.3, 129.2, 129.1, 128.9, 128.7, 128.6, 128.4, 128.1, 127.9, 127.7, 126.8, 126.7, 126.1, 125.9, 125.7, 125.4, 124.5, 124.3, 123.5, 122.8, 56.3, 56.1, 52.5, 52.1, 28.5, 24.1, 23.7. FT-IR (cm^{-1}): 3024 (m), 2849 (m), 1664 (*v* (C=N), m), 1635 (*v* (C=N), m), 1598 (m), 1492 (s), 1448 (s), 1252 (m), 1079 (m), 1030 (m), 906 (w), 859 (m), 831 (s),754 (s), 697 (s). Anal. Calcd. For $C_{69}H_{58}N_2$ (915.21): C, 90.55; H, 6.39; N, 3.06. Found: C, 90.29; H, 6.64; N, 2.89.

L4. Based on the method described for **L1**, **L4** was prepared by the reaction of 1-(2,4,6-tribenzhydrylphenylimino)acenaphthylenone (0.74 g, 1.0 mmol) with 2,4,6-trimethylaniline (0.14 g, 1.2 mmol) in the presence of *p*-toluenesulfonic acid (0.10 g) and isolated as a yellow powder (0.27 g, 31%). Mp: 228–230 ºC. ^{1}H NMR (400 MHz, $CDCl_3$, TMS): δ(ppm) 7.70 (d, J = 8.0 Hz, 1H), 7.56 (d, J = 8.0 Hz, 1H), 7.11–7.28 (m, 15H), 7.09–7.11 (m, 4H), 6.98–7.06 (m, 6H), 6.90–6.94 (m, 1H), 6.82–6.84 (m, 4H), 6.76 (s, 2H), 6.49–6.53 (m, 4H), 6.33–6.37 (m, 2H), 5.61 (s, 2H), 5.43 (s, 1H), 2.39 (s, 3H), 2.18 (s, 6H). ^{13}C NMR ($CDCl_3$, 100 MHz, ppm): δ 163.9, 161.5, 147.8, 146.7, 144.4, 143.2, 139.9, 138.7, 132.9, 132.3, 129.8, 129.7, 129.4, 129.3, 129.2, 129.0, 128.9, 128.7, 128.5, 128.4, 128.1, 127.9, 127.6, 127.4, 126.6, 126.5, 126.0, 125.9, 125.3, 124.6, 124.1, 121.7, 56.3, 52.2, 20.9, 18.0. FT-IR (cm^{-1}): 3057 (w), 3025 (m), 2869 (m), 1667 (*v* (C=N), m), 1638 (*v* (C=N), m), 1595 (m), 1493 (s), 1256 (m), 1231(m), 1153 (m), 1127 (m), 1031 (m), 921 (w), 853 (m), 831 (s),782 (s), 759 (m), 737 (m), 694 (s). Anal. Calcd. For $C_{66}H_{52}N_2$ (873.13): C, 90.79; H, 6.00; N, 3.21. Found: C, 90.59; H, 6.14; N, 3.11.

L5. Based on the method described for **L1**, **L5** was prepared by the reaction of 1-(2,4,6-tribenzhydrylphenylimino)acenaphthylenone (0.74 g, 1.0 mmol) with 2,6-diethyl-4-methylaniline (0.20 g, 1.2 mmol) in the presence of *p*-toluenesulfonic acid (0.10 g) and isolated as an orange powder (0.20 g, 26%). Mp: 220–222 ºC. ^{1}H NMR (400 MHz, $CDCl_3$, TMS): δ(ppm) 7.67 (d, J = 8.4 Hz, 1H), 7.51 (d, J = 8.4 Hz, 1H), 7.11–7.24 (m, 16H), 6.97–7.09 (m, 9H), 6.86–6.88 (m, 1H), 6.81–6.83 (m, 4H), 6.76 (s, 2H), 6.48–6.51 (m, 2H), 6.31–6.34(m, 4H), 5.62 (s, 2H), 5.43 (s, 1H), 2.59–2.68 (m, 2H), 2.46–2.53 (m, 2H), 2.42 (s, 3H), 1.15 (t, J = 7.6 Hz, 6H). ^{13}C NMR ($CDCl_3$, 100 MHz, ppm): δ 163.9, 161.7, 147.8, 145.8, 144.8, 143.4, 142.6, 141.6, 140.3, 139.9, 138.7, 132.9, 132.3, 130.5, 129.8, 129.7, 129.5, 129.4, 129.3, 129.2, 129.1, 128.9, 128.7, 128.4, 128.1, 127.9, 127.8, 127.6, 127.2, 127.0, 126.6, 126.5, 126.0, 125.9, 125.7, 125.3, 124.2, 122.3, 56.3, 56.1, 52.5, 52.2, 24.5, 21.2, 14.5. FT-IR (cm^{-1}): 3056 (w), 3025 (m), 2866 (m), 1666 (*v* (C=N), m), 1636 (*v* (C=N), m), 1596 (m), 1493 (s), 1445 (s), 1252 (m), 1154 (w), 1127 (w), 1077 (m), 1031 (m), 921 (w), 859 (m), 831 (s),783 (s), 744 (m), 694 (s). Anal. Calcd. For $C_{68}H_{56}N_2$ (901.19): C, 90.63; H, 6.26; N, 3.11. Found: C, 90.31; H, 6.38; N, 3.05.

Synthesis of the 1-(2,4,6-tribenzhydrylphenylimino)-2-aryliminoacenaphthene-nickel(II) bromides, Ni1 – Ni5

Ni1. **L1** (0.17 g, 0.20 mmol), (DME)$NiBr_2$ (0.056 g, 0.18 mmol) and dichloromethane (10 mL) were stirred at room temperature for 24 h. The solution was concentrated and diethyl ether (20 mL) added to precipitate the resulting product. Following filtration, the solid was further washed with diethyl ether affording **Ni1** and isolated as a red powder (0.18 g, 93%). ^{1}H NMR (400 MHz, CD_2Cl_2, TMS): δ(ppm) 29.57 (1H, -C*H*Ph_2), 28.89 (6H, -CH_3), 25.82 (2H, Ar-H_m), 24.78 (1H, An-*H*), 22.44 (2H, Ar-H_m), 20.22 (1H, An-*H*), 16.67 (1H, An-*H*), 15.91 (1H, An-*H*), 11.66 (2H, -C*H*Ph_2), 8.51 (Ar-*H*), 8.29 (Ar-*H*), 8.15 (Ar-*H*), 7.63 (Ar-*H*), 7.28 (Ar-*H*), 7.02 (Ar-*H*), 6.09 (1H, An-*H*), 5.52 (Ar-*H*), 5.17 (Ar-*H*), 4.84 (1H, An-*H*), –16.80 (1H, Ar-H_p). FT-IR (cm^{-1}): 3023 (m), 2866 (m), 1645 (*v* (C=N), m), 1620 (*v* (C=N), m), 1586 (m), 1493 (s), 1444 (s), 1296 (m), 1230 (w), 1195 (w), 1130 (w), 1078 (m), 1030 (m), 916 (w), 827 (m), 764 (s), 739 (m), 696 (s). Anal. Calcd. For $C_{65}H_{50}N_2Br_2Ni$ (1077.61): C, 72.45; H, 4.68; N, 2.60. Found: C, 72.35; H, 4.66; N, 2.65.

Ni2. Based on the procedure outlined for **Ni1**, **Ni2** was synthesized by reacting **L2** (0.18 g, 0.20 mmol) with (DME)$NiBr_2$ (0.056 g, 0.18 mmol) and isolated as a red powder (0.14 g, 71%). ^{1}H NMR (400 MHz, CD_2Cl_2, TMS): δ(ppm) 30.01 (1H, -C*H*Ph_2), 28.79 (2H, -CH_2CH$_3$), 26.62 (2H, -CH_2CH$_3$), 25.65 (2H, Ar-H_m), 25.03 (1H, An-*H*), 22.76 (2H, Ar-H_m), 20.33 (1H, An-*H*), 16.68 (1H, An-*H*), 15.98 (1H, An-*H*), 11.41 (2H, -C*H*Ph_2), 8.54 (Ar-*H*), 8.28 (Ar-*H*), 8.15 (Ar-*H*), 7.63 (Ar-*H*), 7.16 (Ar-*H*), 7.00 (Ar-*H*), 6.08 (1H, An-*H*), 5.60 (Ar-*H*), 5.20 (Ar-*H*), 4.85 (1H, An-*H*),0.78 (6H, -CH_2CH$_3$),–16.02 (1H, Ar-H_p). FT-IR (cm^{-1}): 3026 (m), 2868 (m), 1643 (*v* (C=N), m), 1620 (*v* (C=N), m), 1580 (m), 1493 (s), 1447 (s), 1331 (w), 1295 (w), 1252 (w), 1184 (w), 1128 (w), 1076 (m), 1029 (m), 953 (w), 913 (w), 824 (m), 765 (s), 741 (m), 691 (s).

Anal. Calcd. For $C_{67}H_{54}N_2Br_2Ni$ (1105.66): C, 72.78; H, 4.92; N, 2.53. Found: C, 72.86; H, 4.85; N, 2.51.

Ni3. Based on the procedure outlined for **Ni1**, **Ni3** was synthesized by reacting **L3** (0.18 g, 0.20 mmol) with (DME)$NiBr_2$ (0.056 g, 0.18 mmol) and isolated as a red powder (0.15 g, 75%). ^{1}H NMR (400 MHz, CD_2Cl_2, TMS): δ(ppm) 29.90 (1H, -C*H*Ph_2), 24.50 (3H, Ar-H_m, An-*H*), 22.38 (2H, Ar-H_m), 20.43 (1H, An-*H*), 16.51 (1H, An-*H*), 15.57 (1H, An-*H*), 11.51 (2H, -C*H*Ph_2), 8.10 (Ar-*H*), 7.68 (Ar-*H*), 7.16 (Ar-*H*), 6.74 (Ar-*H*), 6.55 (Ar-*H*), 6.24 (1H, An-*H*), 4.80 (Ar-*H*), 4.44 (1H, An-*H*), 0.96 (12H, -C*H*$(CH_3)_2$), –15.65 (1H, Ar-H_p). FT-IR (cm^{-1}): 3039 (w), 2971 (m), 1642 (*v* (C=N), m), 1614 (*v* (C=N), m), 1577 (m), 1495 (s), 1445 (s), 1416 (w), 1294 (w), 1182 (w), 1053 (m), 959 (w), 912 (w), 881 (m), 808 (m), 770 (s), 743 (m), 700 (s). Anal. Calcd. For $C_{69}H_{58}N_2Br_2Ni$ (1133.71): C, 73.10; H, 5.16; N, 2.47. Found: C, 73.14; H, 5.18; N, 2.69.

Ni4. Based on the procedure outlined for **Ni1**, **Ni4** was synthesized by reacting **L4** (0.17 g, 0.20 mmol) with (DME)$NiBr_2$ (0.056 g, 0.18 mmol) and isolated as a brown powder (0.16 g, 83%). ^{1}H NMR (400 MHz, CD_2Cl_2, TMS): δ(ppm) 33.69 (3H, Ar-p-C*H*$_3$), 29.11 (1H, -C*H*Ph_2), 28.40 (6H, -C*H*$_3$), 25.21 (3H, Ar-H_m, An-*H*), 22.07 (2H, Ar-H_m), 20.22 (1H, An-*H*), 16.49 (1H, An-*H*), 15.76 (1H, An-*H*), 10.69 (2H, -C*H*Ph_2), 8.45 (Ar-*H*), 8.23 (Ar-*H*), 8.12 (Ar-*H*), 7.61 (Ar-*H*), 7.26(Ar-*H*), 7.16(Ar-*H*), 6.27(1H, An-*H*), 5.54 (Ar-*H*), 5.17 (Ar-*H*), 4.83(1H, An-*H*). FT-IR (cm^{-1}): 3025 (w), 2914 (m), 1647 (*v* (C=N), m), 1614 (*v* (C=N), m), 1581 (m), 1494 (s), 1444 (s), 1294 (w), 1233 (w), 1188 (w), 1158 (w), 1075 (m), 1130 (w), 913 (w), 862 (m), 826 (m), 801 (w), 769 (s), 738 (m), 696 (s). Anal. Calcd. For $C_{66}H_{52}N_2Br_2Ni$ (1091.63): C, 72.62; H, 4.80; N, 2.57. Found: C, 72.78; H, 4.69; N, 2.59.

Ni5. Based on the procedure outlined for **Ni1**, **Ni5** was synthesized by reacting **L5** (0.18 g, 0.20 mmol) with (DME)$NiBr_2$ (0.056 g, 0.18 mmol) and isolated as a red powder (0.12 g, 60%). ^{1}H NMR (400 MHz, CD_2Cl_2, TMS): δ(ppm) 33.83 (3H, Ar-p-C*H*$_3$), 29.55 (1H, -C*H*Ph_2), 28.31 (2H, -C*H*$_2$CH$_3$), 26.22 (2H, -C*H*$_2$CH$_3$), 25.44 (2H, Ar-H_m), 25.07 (1H, An-*H*), 22.27 (2H, Ar-H_m), 19.89 (1H, An-*H*), 16.53 (1H, An-*H*), 15.87 (1H, An-*H*), 10.18 (2H, -C*H*Ph_2), 8.47 (Ar-*H*), 8.29 (Ar-*H*), 8.19 (Ar-*H*), 7.62 (Ar-*H*), 7.24 (Ar-*H*), 7.07 (Ar-*H*), 6.23 (1H, An-*H*), 5.65 (Ar-*H*), 5.48 (Ar-*H*), 4.83 (1H, An-*H*), 0.87 (6H, -C*H*$_2$CH$_3$). FT-IR (cm^{-1}): 3027 (w), 2962 (m), 1648 (*v* (C=N), m), 1614 (*v* (C=N), m), 1588 (m), 1493 (s), 1449 (s), 1338 (w), 1294 (w), 1260 (w), 1198 (w), 1156 (w), 1129 (w), 1081 (m), 1129(w), 959 (w), 912 (w), 867 (m), 825 (m), 799 (w), 770 (s), 746 (m), 699 (s). Anal. Calcd. For $C_{68}H_{56}N_2Br_2Ni$ (1119.69): C, 72.94; H, 5.04; N, 2.50. Found: C, 73.02; H, 4.94; N, 2.43.

X-ray Crystallographic Studies

Single crystals of **Ni1** and **Ni3** were obtained by slow diffusion of diethyl ether into dichloromethane solutions of the corresponding complex at room temperature. The single-crystal X-ray diffraction studies were carried out on a Rigaku Saturn 724$^+$ CCD with graphite-monochromatic Mo-Kα radiation (λ = 0.71073 Å) at 173(2) K, the cell parameters were obtained by global refinement of the positions of all collected reflections. Intensities were corrected for Lorentz and polarization effects and empirical absorption. The structure was solved by direct methods and refined by full-matrix least squares on F^2. All hydrogen atoms were placed in calculated positions. Structure solution and refinement were performed by using the Olex2 1.2 package.[19] Details of the crystal data and structure refinements for **Ni1** and **Ni3** are shown in Table 8.

Table 8. Crystal data and structure refinements for **Ni1** and **Ni3**

	Ni1	**Ni3**
Empirical formula	$C_{65}H_{50}N_2Br_2Ni$	$C_{69}H_{58}N_2Br_2Ni$
Formula weight	1077.56	1133.70
Temperature/K	173(2)	446(2)
Wavelength/Å	0.71073	0.71073
Crystal system	Monoclinic	Monoclinic
Space group	Cc	P21/c
a/Å	10.302(2)	15.579(3)
b/Å	19.200(4)	20.196(4)
c/Å	25.761(5)	21.046(4)
Alpha/°	90	90
Beta/°	93.99(3)	94.22(3)
Gamma/°	90	90
Volume/Å^3	5083.2(18)	6604(2)
Z	4	4
Dcalcd/(g·cm^{-3})	1.408	1.140
μ/mm^{-1}	1.998	1.541
F(000)	2208	2336
Crystal size/mm	0.35 × 0.24 × 0.09	0.23 × 0.13 × 0.10
θ Range (º)	1.58–27.50	1.31–27.41
Limiting indices	–13 ≤ h ≤ 13	–20 ≤ h ≤ 20
	–24 ≤ k ≤ 24	–26 ≤ k ≤ 26
	–33 ≤ l ≤ 33	–27 ≤ l ≤ 27
No. of rflns collected	31739	84415
No. unique rflns	11545	14955
R(int)	0.0490	0.1294
No. of params	631	671
Completeness to ϑ	99.9 %	99.6 %
Goodness of fit on F^2	1.062	1.124
Final R indices [I >2∑(I)]	R1 = 0.0778	R1 = 0.0944
	wR2 = 0.2153	wR2 = 0.2417
R indices (all data)	R1 = 0.0875	R1 = 0.1232
	wR2 = 0.2374	wR2 = 0.2632
Largest diff. peak, and hole/(e Å^{-3})	0.916 and –1.283	1.130 and –0.727

Ethylene Polymerization

Ethylene polymerization at 1 atm ethylene pressure. Ni1 (0.0021 g, 0.002mmol) was added to a Schlenk vessel, equipped with stir bar, followed by freshly distilled toluene (30 mL). The required amount of co-catalyst, Et_2AlCl (0.4 mmol) or Me_2AlCl (1.4 mmol), was then added by syringe. The reaction mixture was stirred at 1 atm of ethylene pressure at room temperature. After 30 min, the reaction was quenched with 10% hydrochloric acid in ethanol. The polymer was washed with ethanol, then dried under reduced pressure at 60 ºC and weighed.

Ethylene polymerization at 5/10 atm ethylene pressure. The higher pressure polymerization runs were carried out in stainless steel autoclave (0.25 L) equipped with an ethylene pressure control system, a mechanical stirrer and a temperature controller. At the selected reaction temperature, freshly distilled toluene (30 mL) was injected into the autoclave, followed by the complex (2.0 μmol) dissolved in toluene (50

mL). The required amount of co-catalyst (MAO, MMAO, $AlEtCl_2$, EASC, Et_2AlCl, Me_2AlCl, Et_3Al, Me_3Al) was then injected and finally more toluene (20 mL) introduced. The autoclave was immediately pressurized to the designated ethylene pressure and the stirring commenced. After the required reaction time, the ethylene pressure was released, the polymer washed with ethanol and then dried under reduced pressure at 60 ºC and weighed.

Acknowledgements

This work is supported by the National Natural Science Foundation of China (Nos.51373176, 21374123 andU1362204). G.A.S. thanks the Chinese Academy of Sciences for a President's Visiting Scientist Fellowship.

Notes and references

1 W. A. Braunecker, K.Matyjaszewski, *Prog. Polym. Sci.*, 2007, **32**, 93.
2 M. Akiba, A. S. Hashim, *Prog. Polym. Sci.*, 1997, **22**, 475.
3 B. Adhikari, D. De, S. Maiti, *Prog. Polym. Sci.*,2000, **25**, 909.
4 (a) L. R. Kucera, M. R. Brei, R. F. Storey, *Polymer*, 2013, **54**, 3796; (b) X. Xia, Z. Ye, S. Morgan, J. Lu, *Macromolecules*, 2010, **43**, 4889; (c) L. R. Hutchings, J. M. Dodds, D. Rees, S. M. Kimani, J. J. Wu, E. Smith, *Macromolecules*, 2009, **42**, 8675; (d) J. S. Shim, J. P. Kennedy, *J.Polym. Sci. Pol. Chem.*, 2000, **38**, 279; (e) E. Espinosa, B. Charleux, F. D'Agosto, C. Boisson, R. Tripathy, R. Faust, C. Soulie-Ziakovic, *Macromolecules*, 2013, **46**, 3417; (f) W. Wang, R. Schlegel, B. T. White, K. Williams, D. Voyloy, C. A. Steren, A. Goodwin, E. B. Coughlin, S. Gido, M. Beiner, K. Hong, N.-G. Kang, J. Mays, *Macromolecules*, 2016, **49**, 2646; (g) W. Shi, N. A. Lynd, D Montarnal, Y. Luo, G. H. Fredrickson, E. J. Kramer, *Macromolecules*, 2014, **47**, 2037.
5 (a) C. Lee, S. P. Gido, *J. Chem. Phys.*, 1997, **22**, 6460; (b) H. Iatrou, J. W. Mays, N. Hadjichristidis, *Macromolecules*, 1998, **31**, 6697; (c) D. Uhrig, J. W. Mays, *Macromolecules*, 2002, **35**, 7182; (d) I. Chalari, N. Hadjichristidis, *J. Polym. Sci. Pol. Chem.*, 2002, **40**, 1519.
6 (a) H. L. Lu, S. Hong, T. C. Chung, *Macromolecules*, 1998, **31**, 2028; (b) D. J. Arriola, E. M. Carnahan, P. D. Hustad, R. L. Kuhlman, T. T. Wenzel, *Science*, 2006, **312**, 714.
7 (a) L. K. Johnson, C. M. Killian, M. Brookhart, *J. Am. Chem. Soc.*, 1995, **117**, 6414; (b) C. M. Killian, D. J. Tempel, L. K. Johnson, M. Brookhart, *J. Am. Chem. Soc.*, 1996, **118**, 11664; (c) Z. B. Guan, P. M. Cotts, E. F. McCord, S. J. McLain, *Science*, 1999, **283**, 2059; (d) Z. Dong, Z. Ye, *Polym. Chem.*, 2012, **3**, 286; (e) W. C. Anderson, J. L. Rhinehart, A. G. Tennyson, B. K. Long, *J. Am. Chem. Soc.*, 2016, **138**, 774; (f) W. C. Anderson, B. K. Long, *ACS Macro Lett.*, 2016, **5**, 1029.
8 (a) D. Jia, W. Zhang, W. Liu, L. Wang, C. Redshaw, W.-H. Sun, *Catal. Sci. Technol.*, 2013, **3**, 2737; (b) S. Kong, K. Song, T. Liang, C.-Y. Guo, W.-H. Sun, C. Redshaw, *Dalton Trans.*, 2013, **42**, 9176; (c) C. Wen, S. Yuan, Q. Shi, E. Yue, D. Liu, W.-H. Sun, *Organometallics*, 2014, **33**, 7223; (d) S. Du, Q. Xing, Z. Flisak, E. Yue, Y. Sun, W.-H. Sun, *Dalton Trans*., 2015, **44**, 12282; (e) S. Du, S. Kong, Q. Shi, J. Mao, C. Guo, J. Yi, T. Liang, W.-H. Sun, *Organometallics*, 2015, **34**, 582; (f) G. Leone, M. Mauri, I. Pierro, G. Ricci, M. Canetti, F. Bertini, *Polymer*, 2016, **100**, 37; (g) K. S. O'Connor, A. Watts, T. Vaidya, A. M. LaPointe, M. A. Hillmyer, G. W. Coates, *Macromolecules*, 2016, **49**, 6743; (h) X. Wang, L. Fan, Y. Yuan, S. Du, Y. Sun, G. A. Solan, C.-Y.Guo, W.-H. Sun, *Dalton Trans.*, 2016, **45**, 18313; (i) Y. Chen, S. Du, C. Huang, G. A. Solan, X. Hao, W.-H. Sun, *J. Polym. Sci., Part A: Polym. Chem*., 2017, **55**, DOI:10.1002/pola.28562; (j) Y. Zeng, Q. Mahmood, X. Hao, W.-H. Sun, *J. Polym. Sci*., *Part A: Polym. Chem*., 2017, **55**, DOI: 10.1002/pola.28563.
9 (a) H. Liu, W. Zhao, X. Hao, C. Redshaw, W. Huang, W.-H. Sun, *Organometallics*, 2011, **30**, 2418; (b) S. Kong, C.-Y. Guo, W. Yang, L. Wang, W.-H. Sun, R. Glaser, *J. Organomet. Chem.*, 2013, **725**, 37; (c) L. Fan, S. Du, C.-Y. Guo, X. Hao, W.-H. Sun, *J. Polym. Sci. Part A: Polym. Chem.*, 2015, **53**, 1369.
10 (a) H. Liu, W. Zhao, J. Yu, W. Yang, X. Hao, C. Redshaw, L. Chen, W.-H. Sun, *Catal. Sci. Technol.*, 2012, **2**, 415; (b) L. Fan, E. Yue, S. Du, C.-Y. Guo, X. Hao, W.-H. Sun, *RSC Adv.*, 2015, **5**, 93274; (c) W. Zhao, E. Yue, X. Wang, W. Yang, Y. Chen, X. Hao, X. Cao, W.-H. Sun, *J. Polym. Sci. Part A: Polym. Chem.*, 2017, **55**, 988.
11 (a) J. L. Rhinehart, L. A. Brown, B. K. Long, *J. Am. Chem. Soc*., 2013, **135**, 16316; (b) J. L. Rhinehart, N. E. Mitchell, B. K. Long, *ACS Catal.*, 2014, **4**, 2501.
12 (a) E. Yue, L. Zhang, Q. Xing, X.-P. Cao, X. Hao, C. Redshaw, W.-H. Sun, *Dalton Trans*., 2014, **43**, 423; (b) F. Huang, Z. Sun, S. Du, E. Yue, J. Ba, X. Hu, T. Liang, G. B. Galland, W.-H. Sun, *Dalton Trans*., 2015, **44**, 14281; (c) C. Huang, Y. Zhang, T. Liang, Z. Zhao, X. Hu, W.-H. Sun, *New J. Chem.*, 2016, **40**, 9329.
13 G. B. Galland, R. F. De Souza, R. S. Mauler, F. F. Nunes, *Macromolecules*, 1999, **32**, 1620.
14 (a) S. A. Svejda, L. K. Johnson and M. Brookhart, *J. Am. Chem. Soc.*, 1999, **121**, 10634; (b) D. J. Tempel, L. K. Johnson, R. L. Huff, P. S. White and M. Brookhart, *J. Am. Chem. Soc.*, 2000, **122**, 6686; (c) L. H. Shultz, D. J. Tempel, M. Brookhart, *J. Am. Chem. Soc.*, 2001, **123**,11539; (d) K. E. Allen, J. Campos, O. Daugulis, M. Brookhart, *ACS Catal.*, 2015, **5**, 456; (e) M. D. Leatherman, S. A. Svejda, L. K. Johnson, M. Brookhart, *J. Am. Chem. Soc.*, 2003, **125**, 3068; (f) I. E. Soshnikov, N. V. Semikolenova, K. P. Bryliakov, V. A. Zakharov, W.-H. Sun, E. P. Talsi, *Organometallics*, 2015, **34**, 3222; (g) A. A. Antonov, N. V. Semikolenova, E. P. Talsi, M. A. Matsko, V. A. Zakharov, K. P. Bryliakov, *J. Organomet. Chem.*, 2016, **822**, 241; (h) Y. Zhang, C. Huang, X. Wang, Q. Mahmood, X. Hao, X. Hu, Cu.-Y.Guo, G. A. Solan, W.-H. Sun, *Polym. Chem.*, 2017, **8**, 995.
15 (a) G. R. Hamed, N. R.Attanasom, *Rubber Chem. Technol.*, 2002, **75**, 935; (b) B. Gabrielle, L. Guy, P.-A. Albouy, L. Vanel, D. R. Long, P. Sotta, *Macromolecules*, 2011, **44**, 7006.
16 Y. Kong, J. N. Hay, *Polymer*, 2002, **43**, 3873.
17 T. Usami, S. Takayama, *Polym. J.*, 1984, **16**, 731.
18 Z. He, Y. Liang, W. Yang, H. Uchino, J. Yu, W.-H. Sun, C. C. Han, *Polymer*, 2015, **56**, 119.
19 O. V. Dolomanov, L. J. Bourhis, R. J. Gildea, J. A. K. Howard, H. Puschmann, *J. Appl. Cryst.*, 2009, **42**, 339.